# Estimating the Rician Noise Level in Brain MR Image

María G. Pérez[a], Aura Conci[b], Ana Belén Moreno[c], Víctor H. Andaluz[a] and Juan A. Hernández[d]

[a]FISEI, Universidad Técnica de Ambato, Ambato, Ecuador, {mg.perez, victorhandaluz}@uta.edu.ec,
[b]Universidade Federal Fluminense (UFF), 24210-240 Niteroi, Brazil, aconci@ic.uff.br
[c]Universidad Rey Juan Carlos (URJC), 28933 Móstoles, Madrid, Spain, belen.moreno@urjc.es
[d]Alzheimer Center, Reina Sofía Foundation, 28006 Madrid, Spain, juan.tamames@urjc.es

***Abstract*- Estimation of the noise level in images is very important to assess the quality of the acquisition and to allow an efficient analysis. Moreover, it is a fundamental step, an indispensable procedure for many type of denoises and image processing. In this paper a new method to estimate the noise level in MR images is presented and evaluated. The advantage of this is the easiness for utilization during image acquisition and of course the adaptability of the idea of other areas of body. The correctness of the evaluation is addressed by comparison of Atlas noise free images where the level of Rician noise was artificially added and known. The main idea is the matching of same slices after registration in order to evaluate the level of noise. For evaluation of the range of noise in an image we used the signal noise ratio – SNR and a set of MRI with increasing levels of Rician noise. However, others metrics like the normalized cross correlation - NCC or the Root Mean Squared Error (RMSE) could be used as well.**

**Keyworks-MRI brain atlas; Rician noise; image registration; signal noise ratio, interpolation.**

## I. INTRODUCTION

Medical diagnosis by Magnetic Resonance (MR) have become of great importance. However the used of good images is a critical aspect in such application of image processing. Despite significant improvements in recent years, magnetic resonance images (MRI) obtained directly by the instruments are frequently inadequate by medical analysis, especially in cardiac and brain [1] images because they present high levels of Rician noise [2][3]. Although, many image processing techniques could improvement the image quality by filtering or sharpening it, the acknowledgement of the quantity of noise present in these is fundamental for adequate de-noising design. Usually, the real and imaginary parts of the MR complex raw data are considered corrupted by white additive Gaussian noise, where the noise variance is assumed to be the same in both parts (real and imaginary). By taking the magnitude of the complex data, the noise is transformed into Rician noise. Noise in magnitude MR images can be well modeled by a Rician distribution when computed from a single complex raw data as well. Rician noise introduces a bias into MRI measurements that can have an impact on the shapes and orientations of tensors in functional (or diffusion) magnetic resonance images. This is less problematical in structural MRI, because this bias is signal dependent and it does not seriously affect tissue recognition. However, functional MRI (or diffusion) imaging is used extensively for quantitative evaluations, and in these, a good estimation of the level of Rician noise present is a very important aspect.

This work presents new noise estimation approach that is easily used in the medical environment during the acquisition process because it is based in simple computation and comparison of a previous organized Table. It has the advantage to be specially designed to brain images and Rician noise, as well. The main proposition is the use of registration and evaluation of the signal noise ratio of the real image with unknown level of noise based on comparison with a specially generated Table of artificially known noise added in synthetic noise free images of the similar type. The obtained results are compare with other works on the same propose.

Thanks to CAPES agency for founding in part the Brazilian author of this work. We also thank the UTA-Ecuador Research Project 2340-CU-P-2013.

## II. THE RICIAN NOISE PRESENTED IN MRI

The noise models in magnitude MRI have been considered in [4][5]. The Rician distribution, showed in Figure 1, gives the best overall description in such images when they are computed from a single complex raw data [3]:

$$p(m) = \frac{m}{s_n^2}\exp\left(-\frac{m^2+A^2}{2s_n^2}\right) I_0\left(\frac{Am}{s_n^2}\right) \quad (1)$$

where $s_n$ is the standard deviation (StD) of Gaussian noise in the complex domain, $\boldsymbol{m}$ is the value in the magnitude image an $I_0$ is the zero[th] order modified Bessel function [3]. $A$ is the amplitude of the signal without noise and is given by: $\boldsymbol{A^2 = A^2_R + A^2_I}$, where $\boldsymbol{A_R}$ and $\boldsymbol{A_I}$ are respectively the real and imaginary data. It is important to note that the Rice distribution ends to a Rayleigh distribution when the signal to noise ratio goes to zero (i.e., $\boldsymbol{A}/s_n \rightarrow 0$), as Figure 1 presents. Rician distribution is signal dependent and consequently it is difficult to separate signal from the noise. Rician noise is especially problematic in low quality images, or images with

low SNR (Figure 1). It introduces signal dependent bias to the data that reduces image contrast, as well.

The noise level in an image may be determined in several ways. It can be measured directly from a large uniform, signal region as the standard deviation of pixel values in that region. Another approach which may be employed on magnitude reconstructed images is noise estimation from the signal amplitude value of non signal regions [6]. Alternatively, the noise can be determined by acquiring two images of the same object, subtracting one from the other and finding the standard deviation of the difference image. This last technique is the one currently advocated by National Electrical Manufacturers Association (NEMA) [6]. It has an advantage over the first two techniques of evaluation of noise: When properly employed, it is relatively insensitive to structured noise, for example, noise due to phenomena such as ghosting, ringing across edge boundaries due to finite sampling, and so on. A simple approach to estimate the Rician noise variance is to use the difference between two matched images of the same object [7]. Murphy et al., 1993 have developed a parallel rod test object (PRoTO) and a set of computer implemented analysis programs for noise estimation [7]. An image of the cross section of the PRoTO has a checker board appearance consisting of signal and non signal blocks. The analysis programs automatically extract many machine performance variables from a set of images of a single scan of the phantom and utilize them in the routine of quality control (QC) [7]. One of the advantages that this phantom and set of analysis routines provides is the easy determination of signal, voxel volume (x ,y pixel sizes and slice thickness), and various measures of noise at many locations within a slice (for each slice) of a single scan. This makes the phantom and programs ideal for exploring the significance of variables incorporated in the SNR. Although the technique is simple to implement, its efficiency relies heavily on the correct alignment of the two images. Therefore, others authors present techniques that use only a single image. The first methods using a single image were based on manual selection of uniform signal or non-signal regions [8][9]. However such techniques are time consuming and have a high intra and inter user variability. Naturally, some automatic techniques have been proposed [10][11][9][12]. Usually, these methods use the histogram of the background and some properties of the Rayleigh distribution. A common manner to measure the Rician noise variance in magnitude MR images with large enough background areas is to estimate it from the mode of the histogram [11][10][9]. A new noise Rician variance estimation method based on maximum likelihood (ML) estimation from a partial histogram was presented [9]. Aja-Fernandez et al. (2008) [12] presented a set of new methods for noise estimation based on local statistics that are able to estimate the noise variance from the background but also from the imaged object in a very simple and efficient manner. Recently, Coupé et al, 2010 [13] propose an adaptation of the Median Absolute Deviation (MAD) estimator in the wavelet domain is proposed for Rician noise. This robust and efficient estimator has been proposed by Donoho (1995) [14] for Gaussian noise and since has been widely used in image processing. Coupé et al, 2010 [13] propose to adapt this operator for Rician noise by using only the wavelet coefficients corresponding to the object and then iteratively correcting the MAD estimation with an analytical scheme based on the SNR of the image [15]. We here propose the use of a simple Table to evaluate the noise level. Such table is constructed from a free of noise atlas where a known level of noise was added on each slice after its registration and then used to evaluate the level of a real image with unknown level of the same type of noise. The advantage of this is the easiness for utilization during image acquisition and of course the adaptability of the idea of other areas of the human body. The correctness of the evaluation is addressed by comparison of images where the level of noise was computed by other approaches.

## III. Proposed Method

The main idea is the use of a table as standard noised brain images of know level for comparison after registration with the same slice where the level of noise must be evaluated. For evaluation of the level of noise we used the signal noise ratio-SNR. However, others metrics like the normalized cross correlation-NCC or the Root Mean Squared Error could be used as well.

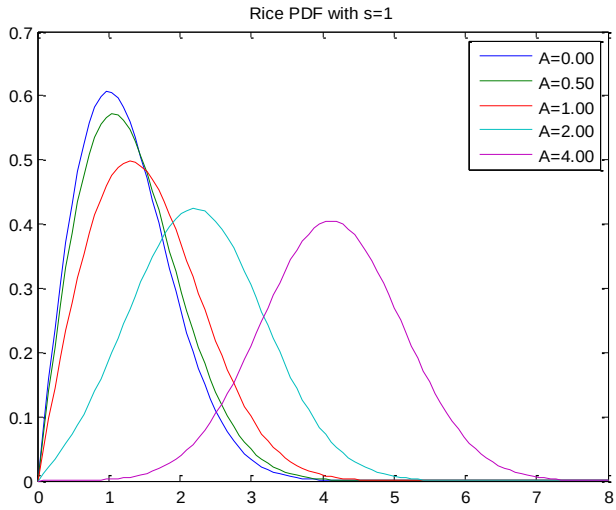


Figure 1. Rice probability density function for different signal magnitude. At SNR = 0 (i.e A/s=0) or at very low SNR, the Rician distribution is approximately a Rayleigh distributed. At low to medium SNR, it is neither Gaussian nor Rayleigh. For high SNR (i.e. SNR>3 or A/s > 3) the Rician data is approximately a Gaussian distribution.

The first part of the proposition is to relate the Rician noise level and the SNR. This is obtained through a series of experimentation adding different levels of noise in gold standard image (i.e. a free of noise image) of brain. These images were normalized between 0 and 255 levels of grey and used to computing their corresponding SNR. Figure 2 shows the main elements for the computation of one element, in this case the slice 72, for the first level of noise, which is second column of Table I. The first image in Figure 2 is the original slice 72 (that we named image **A**). The second image in Figure 2 is the same slice but after the addition of Rician noise, in this case we use it with $\sigma_{noise}$ =10. We name this image **B**: that is $\mathbf{A} + \boldsymbol{\sigma}_{\mathbf{noise}} = \mathbf{B}$. The image on right of Figure

2 is the square of the subtraction image: $(\mathbf{A} - \mathbf{B})^2$ to show the level of noise added to the original slice, **A**, this is used in the denominator of equation 2 for evaluation of the SNR between images **A** and **B**: ***SNR (A, B)***.

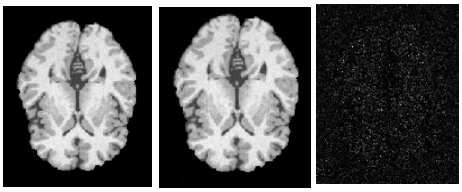

Figure 2. A sample of the how is obtained on element of Table 1: on the right the original image: **A**, on middle it after the addition of Rician noise: **B**, and onthe right is the square of the subtraction image: $(A - B)^2$

On generation of Table I, we here consider as images **A** a set of structural MIR without any initially kind of noise. That is to evaluate the different slices we use a noise free (ground truth) T1 weighted MR data from the Brain Web database [16]. Such data set is composed of eleven (11) slices shown in Figure 3. The BrainWeb [16] dataset used represents classic MRI acquisition parameters: T1-weighting mode, 1 mm slices and resolution of 181 x 217 x 181 voxels. The repetition time (TR) was equal to 18 ms and echo time (TE) was 10ms in an angle of 30 degrees at MINC storage (16 bit little endian format for integers). For the images **B** generation, we corrupted each slice with different levels of Rician noise ($\sigma_{noise}$= 10 to $\sigma_{noise}$= 300) resulting in the level of SNR shown in Table I. The noise was added for each slice after the skull elimination. As the noise added are know, this Table gives a good way to verify the relation among the quality of and image, measured by the **SNR** and the level of noise in such images.

The **Brain isolation (or skull stripping)** is an important step in enabling accurate measurement of brain structures and so it must be done on computing Table I. This allows better execution of registrations and other important aspect of MRI examination, as well. We performed this by using the Brain Extraction Tool (BET) [17]. BET is guided by constraints on surface smoothness and by the voxel intensity nearby the surface position. It is a tool to remove the skull and all the materials that composed the layer between the human brain and the skull (such as hard material, marrow, air, vessels, fat, etc., i.e., all the tissues that are not part of the brain to be analyzed). This tool has been used in a lot of intracranial segmentation methods. It is based on the application of thresholding combined with morphological techniques [17]. BET has been tested on thousands of images, giving accurate segmentation in most of them. It has been conveniently included in FSL [18], MRIcro [19] and mri3dX [20]. We use the MRIcro free software version of this [19] to removal of non-brain tissues.

For addition of the **Rician noise** to the atlas (free of noise) images **(**that is to obtain **B** images) with desired standard deviation value ($\sigma_{noise}$) we use the Tool Rician developed in Mathworks [21].

Naturally, depending on the artificial added degradation (that is levels of Rician standard deviations) and of the slice we obtain various **SNR** by Equation 2. In Table I it is presented for nine levels of Rician added in several slice of the structural MRI for a series we have special interest. We have used the snr.m tool of the WaveLab Tool [22] for this computation. The snr function WavelLab's uses the following definition (Equation 2) by SNR:

$$\mathrm{SNR}\left(\mathrm{Im}_{\mathrm{ref}}, \mathrm{Im}_{\mathrm{noise}}\right) = 10\log_{10}\left(\frac{\left\|\mathrm{Im}_{\mathrm{ref}}\right\|_2}{\left\|\mathrm{Im}_{\mathrm{ref}} - \mathrm{Im}_{\mathrm{nise}}\right\|_2}\right) \qquad (2)$$

where $\boldsymbol{Im_{ref}}$ is the reference image (or signal), $\boldsymbol{Im_{noise}}$ is the noisy image (or signal) and $\|.\|_2$ is the usual $d^2$ norm.

In order to estimate the noise level in a real image the proposed method follows the followings steps (in Figure 4).

**Step 1: Image acquisition, skull stripping and image normalization in 256 levels of grey**- after acquisition of the real image the skull is eliminated in each slice for better comparison with the way Table 1 was performed. Of course this process of skull elimination could be overpass by computing in similar Table with such element. As mentioned before we use the MRIcro free software version of this [19]. The same software used in elaboration of Table 1 must be used to removal non-brain tissues. These images, as those for generation of Table I, were normalized between 0 and 255 levels of grey.

**Step 2: Slices co registration and alignment of the atlas free of noise and the real image -** In the step 1 the two images to be compared must be adjusted before the real SNR of the slices computation. Figure 5 shows the importance of this step. We have used the SPM8 for this [23]. The rigid-body model Coreg is used for this registration. It reslices the images to match the source voxel-for voxel.

**Step 3: Computation of the** SNR of the slices – after matched the noise free slice and the real image slice the SNR of both is computed, it is used in the next step as entry in the Table for identification of the true range of noise of the image.

**Step 4: Evaluation of the noise level –** the slice used and the computed SNR as considered in Table I for identification of the range noise level.

## IV. Experimental Results

In order to verify the proposed method we first used 3 noise free image with known level of noise and then a real image with an unknown level of noise for comparison of our results with other methods in literature. All experiments were realized in a Pentium Intel Pentium 4 CPU 3.00 GHz 2.99 GHz, 1,00 RAM's GB Extension of physical direction and Microsoft Windows XP Professional operational system.

TABLE I. **SNR** RESULTS CONSIDERING THE ATLAS IMAGE (WITHOUT NOISE) AND THE SAME IMAGE WITH RICIAN NOISE ADDED AT NINE LEVELS FROM $\sigma_{noise}$ $\sigma_{noise}$ =10 TO $\sigma_{noise}$ =300

| Slice | $\sigma_{noise} = 10$ | $\sigma_{noise} = 20$ | $\sigma_{noise} = 60$ | $\sigma_{noise} = 100$ | $\sigma_{noise} = 140$ | $\sigma_{noise} = 180$ | $\sigma_{noise} = 220$ | $\sigma_{noise} = 260$ | $\sigma_{noise} = 300$ |
|---|---|---|---|---|---|---|---|---|---|
| **110** | 21.1446 | 18.1269 | 14.0908 | 11.0664 | 8.7653 | 7.2093 | 6.4199 | 5.6405 | 5.3610 |
| **100** | 21.9516 | 17.4776 | 13.6353 | 10.0566 | 8.8190 | 7.3491 | 6.7072 | 5.8290 | 5.3306 |
| **90** | 19.9087 | 19.3155 | 13.9580 | 10.8305 | 9.0761 | 7.9995 | 6.3963 | 5.9813 | 5.2918 |
| **87** | 21.5792 | 17.7763 | 13.9869 | 9.9694 | 8.7432 | 7.5944 | 6.8725 | 5.5427 | 4.8658 |
| **83** | 21.1581 | 18.9588 | 14.5334 | 10.9165 | 8.3858 | 7.3780 | 5.9663 | 5.6909 | 4.8631 |
| **72** | 21.1971 | 19.0970 | 14.3045 | 10.5786 | 8.7371 | 7.3379 | 6.5165 | 5.6011 | 5.4698 |
| **65** | 22.2514 | 16.9874 | 14.5000 | 10.3466 | 8.9815 | 7.2456 | 6.4831 | 5.7283 | 5.2532 |
| **57** | 21.1197 | 17.7713 | 13.6235 | 10.1277 | 8.7691 | 7.5884 | 6.5236 | 5.5513 | 4.9158 |
| **47** | 19.2808 | 16.7890 | 12.1487 | 9.6883 | 8.3974 | 7.0429 | 6.1205 | 5.6831 | 4.8938 |
| **38** | 18.1949 | 15.1159 | 11.2804 | 9.3542 | 8.0330 | 6.7632 | 6.0956 | 5.4222 | 4.8069 |
| **29** | 17.1096 | 14.3130 | 9.7113 | 7.8669 | 6.6304 | 5.7135 | 5.0548 | 4.5395 | 4.1347 |
| **Average SNR μ** | **20.4451** | **17.4299** | **13.2521** | **10.0729** | **8.4853** | **7.2020** | **6.2869** | **5.5645** | **5.0170** |
| St. deviation | 1.6331 | 1.5834 | 1.5484 | 0.9027 | 0.6825 | 0.5870 | 0.4880 | 0.3714 | 0.3805 |
| St. error of the μ: $se_{\bar{x}} = \frac{sd}{\sqrt{n}}$ | **0.4924** | **0.4774** | **0.4669** | **0.2722** | **0.2058** | **0.1770** | **0.1471** | **0.1120** | **0.1147** |

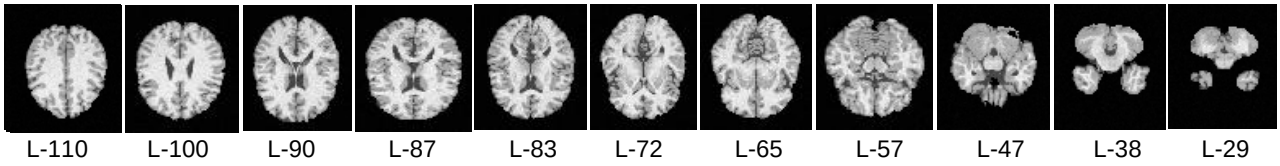


Figure 3. Used slices for Table I computation

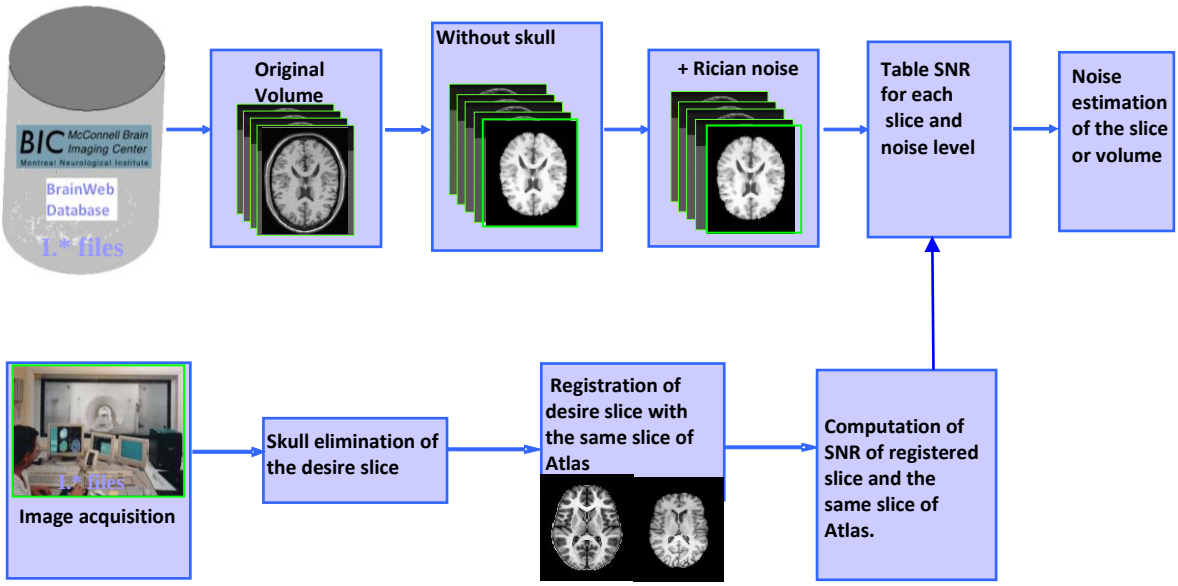


Figure 4. Step of the used proposed noise evaluation methodology.

For the first set of experiments the same atlas was used. In each slice we added noise in the three levels: $\sigma_{noise}$ =90, $\sigma_{noise}$ =160 and $\sigma_{noise}$ =400 and after computation of the SNR the results in the Table II are achieved. Using this results in Table I we can compute, by interpolation, as the average noise level of each image as: 87.9676; 157.02797 and 351.6018 respectively. Figures 6 and 7 show the images used for the case with less noise and greater noise. For the second set of experiments the images on Figure 5 have been used. These get to SNR=5.4082, this correspond in Table I, after extrapolations of values, to a noise level up to $\sigma_{noise}$ =318.7661. Figure 8 shows the original image and the image with noise level of $\sigma_{noise}$ =300 used to generate Table II. We can see that both the visually present the same level of noise.

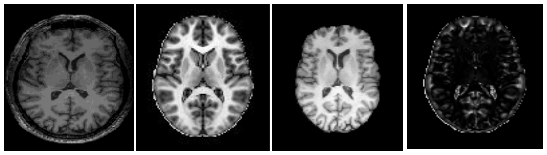

Figure 5. Registraion Step: the slice 72 of real image: C, the slice 72 of the Atlas: D, the same slice of the real image after registration: E and F= $(E-D)^2$ that is used for SNR computation.

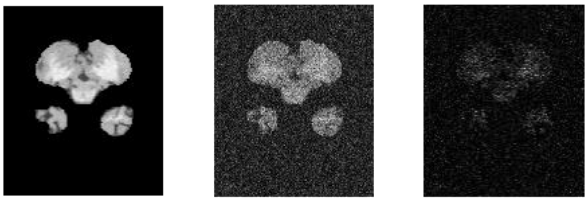

Figure 6. The slice 29 used to compute Table II (left) , the same slice after addition of the higher level of noise ( $\sigma_{noise}$ =400 ) (center) and the square of the subtration of both images (right)

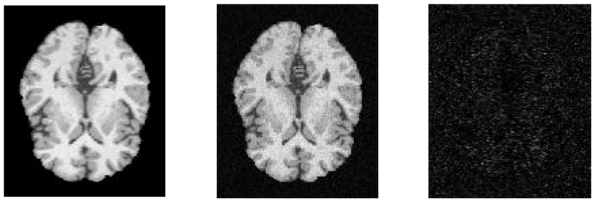

Figure 7. The slice 72 used to compute Table II (left) , the same slice after addition of the lower level of noise ( $\sigma_{noise}$ =90 ) (center) and the square of the subtration of both images (right)

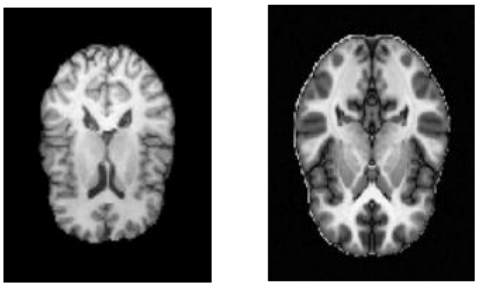

Figure 8. The slice after elimination of the real image with SNR=5.4082 ( $\sigma_{noise}$ > 300 ) , the same slice of the the image with $\sigma_{noise}$ =300 used for composition of Table I.

TABLE II. TYPE SNR RESULTS CONSIDERING THE ATLAS IMAGE (WITHOUT NOISE) AND THE SAME IMAGE WITH RICIAN NOISE ADDED AT NINE LEVELS OF $\sigma_{noise}$ =90, $\sigma_{noise}$ =160 AND $\sigma_{noise}$ =400

| Slice | $\sigma_{noise}$ =90 | $\sigma_{noise}$ =160 | $\sigma_{noise}$ =400 |
|---|---|---|---|
| **110** | 11.5181 | 8.1510 | 4.3632 |
| **100** | 11.6308 | 8.2271 | 4.4215 |
| **90** | 11.6587 | 8.2561 | 4.4562 |
| **87** | 11.6887 | 8.2876 | 4.4892 |
| **83** | 11.6268 | 8.2430 | 4.4613 |
| **72** | 11.6806 | 8.2885 | 4.4952 |
| **65** | 11.6958 | 8.2996 | 4.5081 |
| **57** | 11.5591 | 8.2312 | 4.5038 |
| **47** | 10.4702 | 7.7479 | 4.2375 |
| **38** | 9.6758 | 7.5022 | 4.1457 |
| **29** | 8.1224 | 6.0953 | 3.3363 |
| **Average** | **11.0297** | **7.9390** | **4.3107** |
| Standard deviation | 1.1633 | 0.6638 | 0.3440 |
| Standard error of the mean: $se_{\bar{x}} = \frac{sd}{\sqrt{n}}$ | 0.3507 | 0.2001 | 0.1037 |

## V. CONCLUSION

This work presents an idea for estimation directly the level of Rician noise of images. The idea are been tested in synthetic and real images of Brain MRI. Considering the results obtained using the noise free image added with the level of noise known we can say that the proposed methodology presets the expected values. Comparing the use of the proposition with real image show that this presents adequate results [24]. Of course comparison with other works must be done.


## ACKNOWLEDGMENT

For developing this work the second author receives grants from the Brazilian agencies CAPES and CNPq. We also thank the UTA-Ecuador Research Project 2340-CU-P-2013 and the Spanish Ministry of Science and Innovation Project TIN-29827-C02-01.


## REFERENCES


[1] L.A. Alpuente, A.M. López, R.Y. Tur, "Glioblastoma: changing expectations?", *Clin Transl Oncol*, vol. 13, pp. 240-248, 2011.

[2] J. Sijbers, A.J. den Dekker, J. Van Audekerke, M. Verhoye and D. Van Dyck. "Estimation of the noise in magnitude MR images", *Magnetic Resonance Imaging*, vol. 16, No. 1, pp. 87-90, 1998.

[3] S.O. Rice, "Mathematical analysis of random noise", *Bell Systems Technical Journal*, vol. 23, pp. 282-332, 1944.

[4] S. Basu, T. Fletcher, and R. Whitaker, "Rician noise removal in diffusion tensor MRI", in Proc. MICCAI, vol. 1, pp. 117–125, 2006.

[5] H. Gudbjartsson and S. Patz, "The Rician Distribution of Noisy MRI Data", *Magn Reson Med*.; vol. 34, No 6, pp. 910-914, 1995.

[6] L. Kaufman, D.M. Kramer, L.E. Crooks, D.A. Ortendahl, Measuring signal-to-noise ratios in MR imaging, *Radiology*, vol. 173, pp. 265-267, 1989.

[7] B.W. Murphy, P.L. Carson, J.H. Ellis, Y.T. Zhang, R.J. Hyde, T.L. Chenevert , 1993, Signal-to-noise measures for magnetic resonance images, *Magnetic Resonance Imaging*, vol. 11, No. 3, pp. 425-428.
[8] R.M. Henkelman, "Measurement of signal intensities in the presence of noise in MR images", *Med Phys*, vol. 12, No. 2, pp. 232-233, 1985.
[9] J. Sijbers, D. Poot, A.J. den Dekker, and W. Pintjens, "Automatic estimation of the noise variance from the histogram of a magnetic resonance image, *Phys. Med. Biol*., vol. 52, pp. 1335-48, 2007.
[10] J. Sijbers, A.J. den Dekker, J. Van Audekerke, M. Verhoye and D. Van Dyck, "Estimation of the noise in magnitude MR images", *Magnetic Resonance Imaging*, vol. 16, No. 1, pp. 87-90, 1998.
[11] G. van Kempen, L. van Vliet, "The influence of the background estimation on the superresolution properties of nonlinear image restoration algorithms", D. Cabib, C.J. Cogswell, J-A. Conchello, JM. Lerner, T. Wilson, editors, Three-dimensional and multidimensional microscopy: image acquisition and processing IV, Proceedings of the SPIE Conference, vol. 3605, pp. 179-189, 1999.
[12] S.Aja-Fernandez, C. Alberola-Lopez, C. F. Westin, "Noise and signal estimation in magnitude MRI and Rician distributed images: A LMMSE approach", *IEEE Transactions on image processing*, vol. 17, No. 8, pp. 1383-1398, 2008.
[13] P. Coupé, J.V. Manjón, E. Gedamu, D. Arnold, M. Robles, and D. Louis Collins, "Robust Rician noise estimation for MR images", *Medical Image Analysis*, vol. 14, No. 4, pp. 483-493, 2010.
[14] D.L. Donoho, "De-Noising by Soft-Thresholding", *IEEE Trans. Inform. Theory*, pp. 613-627, 1995.
[15] C.G. Koay and P.J. Basser, "Analytically exact correction scheme for signal extraction from noisy magnitude MR signals". *Journal of Journal of Magnetic Resonance*, vol. 179, pp. 317-322, 2006.
[16] http://www.bic.mni.mcgill.ca/brainweb
[17] S.M. Smith, "Fast robust automated brain extraction". Human Brain Mapping, Vol. 17 No. 3, pp. 143-155, 2002.
[18] http://www.fmrib.ox.ac.uk/fsl/bet2/index.html
[19] MRIcro:http://www.psychology.-nottingham.ac.uk/staff/cr1-/mricro.html
[20] http://cubric.psych.cf.ac.uk/Documentation/mri3dX/download-unsupported-beta-distribution-of-mri3dx/
[21] http://www.mathworks.de/matlabcentral/fx_files/14237/3/content/rician/html/ricedemo.html
[22] http://www-stat.stanford.edu/~wavelab/Wavelab_850/
[23] http://www.fil.ion.ucl.ac.uk/spm/
[24] G. Pérez, A. Conci, A.B. Moreno, J.A. Hernández, "Rician Noise Attenuation in the Wavelet Packet Transformed Domain for Brain MRI", *Integrated Computer-Aided Engineering*, vol. 21, No. 2, pp. 163-175, 2014.